since 1961

Baltica

BALTICA Volume 36 Number 2 December 2023: 115–132
https://doi.org/10.5200/baltica.2023.2.3

A comparison of different machine learning models for landslide susceptibility mapping in Rize (Türkiye)

Hacer Bilgilioğlu*

Bilgilioğlu, H. 2023. A comparison of different machine learning models for landslide susceptibility mapping in Rize (Türkiye). *Baltica*, *36 (2)*, 115–132. Vilnius. ISSN 0067-3064
Manuscript submitted 26 May 2023 / Accepted 15 October 2023 / Available online 14 November 2023

Abstract. The main purpose of this study was to compare the performance and validation of six machine learning models (extreme gradient boosting, random forest, artificial neural network, support vector machine, C4.5 decision tree, and naive Bayes) in landslide susceptibility modelling. The province of Rize, which has the highest rate of landslide events in Türkiye, was chosen as the study area. The conditioning factors (distance to roads, lithology, drainage density, slope, topographic wetness index (TWI), soil depth, distance to rivers, land use, NDVI, plan curvature, elevation, aspect, profile curvature) affecting the landslide were determined using the ReliefF method. A total of 516 landslides were identified for creating models, comparing performance, and validating results. The performance and validation of the models were determined by the receiver operating characteristics (ROC), sensitivity, specificity, accuracy, and kappa index. The results show that the XGBoost model outperforms the other five machine learning models in terms of accuracy and performance and is the most effective model for generating landslide susceptibility maps in Rize (Türkiye).

Keywords: landslide; susceptibility; machine learning; Rize; XGBoost; random forest (RF)

Hacer Bilgilioğlu (hcanbas@aksaray.edu.tr), https://orcid.org/0000-0002-8629-1077
Faculty of Engineering, Department of Geological Engineering, Aksaray University, 68100, Aksaray, Türkiye

INTRODUCTION

Landslides are geological disasters that frequently occur worldwide and cause economic losses as well as severe damage to the natural and artificial environment and human life (Chen *et al.* 2018a; Chen, Yan *et al.* 2019). Different natural events or anthropogenic activities, such as earthquakes, flash floods, road construction, deforestation, and mineral exploration, can trigger landslides, and events such as climate change and population have increased the risk of landslides worldwide (Chen *et al.* 2018b; Pradhan *et al.* 2014). According to the Emergency Events Database (EM-DAT), approximately 40,000 people have lost their lives due to landslides in the last five decades. Using landslide risk assessment studies, disaster prevention and mitigation policies can be developed, and the damage caused by landslides can be reduced by making disaster-oriented plans. One of the essential steps of landslide risk assessment and management is the creation of landslide susceptibility maps that predict and show the spatial likelihood of future landslides (Ercanoglu, Gokceoglu 2002).

Many qualitative and quantitative models have been developed for landslide susceptibility mapping (Dai *et al.* 2002; Youssef *et al.* 2016). Deterministic models based on physical foundations use mechanical laws and require detailed geotechnical and hydrogeological data; therefore, they are unsuitable for large-area studies (Luo, Liu 2018; Pham, Shirzadi *et al.* 2018). In contrast, data-driven quantitative models are preferred for larger study areas because the model is created using only input-output data. These models generally fall into three types: heuristic, statistic, and machine learning (ML). In heuristic methods, a model is created by determining factor importance levels from expert opinions (AlSanea, Abdullah 2021; Huang, Cao *et al.* 2020; Wu *et al.* 2020). The rela-

tionship between landslide inventory and conditioning factors is used in statistical modelling methods, such as the frequency ratio method (Hong *et al.* 2019; Pradhan *et al.* 2014), the linear discriminant model (Youssef, Pourghasemi 2021), the weights-of-evidence method (Kavzoglu *et al.* 2015; Teerarungsigul *et al.* 2016), and the information value method (Che *et al.* 2012; Sarkar *et al.* 2013). With the developments in computer informatics in recent years, many ML models have frequently been used in landslide susceptibility prediction (LSP) studies. The most important advantages of ML models over the other models are their reproducibility and ability to handle multi-faceted factors, update potential, produce more meaningful or accurate results, and process data under uncertain or dynamic conditions (He *et al.* 2012). This type of model includes binary logical regression (Akinci, Zeybek 2021; Bai *et al.* 2021; Huang, Chen *et al.* 2020; Wang *et al.* 2020), decision tree (DT) (Huang, Chen *et al.* 2020), support vector machine (SVM) (Akinci, Zeybek 2021; Kavzoglu, Colkesen 2009; Orhan *et al.* 2022), artificial neural networks (ANN) (Hu *et al.* 2021; Saha, Roy, Hembram *et al.* 2021; Youssef, Pourghasemi 2021; Zhou *et al.* 2018), adaptive neuro-fuzzy inference system (ANFIS) (Chen *et al.* 2017; Chen, Panahi *et al.* 2019), naive Bayes (NB) (Ali *et al.* 2021; Oh *et al.* 2019; Taheri *et al.* 2019), generalized additive model (GAM) (Chen *et al.* 2017; Youssef *et al.* 2016), AdaBoost (AB) (Kadavi *et al.* 2018; Kutlug Sahin, Colkesen 2019, 2021), random forest (RF) (Akinci, Zeybek 2021; Bai *et al.* 2021; Bui *et al.* 2020; Chang *et al.* 2019; Iban, Sekertekin 2022; Kong *et al.* 2021; Orhan *et al.* 2022; Sahin *et al.* 2018), classification and regression tree (CART) (Orhan *et al.* 2022; Saha, Roy, Hembram *et al.* 2021; Youssef *et al.* 2016), multivariate adaptive regression splines (MARS) (Youssef, Pourghasemi 2021), rotation forest (Kutlug Sahin, Colkesen 2021; Saha, Roy, Pradhan *et al.* 2021).

Although many models are frequently used in the literature, there is no consensus on the most appropriate or best model. Further comparison of different ML methods is critical to improving landslide susceptibility modelling (Pham, Prakash *et al.* 2018). Although naive Bayes (NB), artificial neural network (ANN), support vector machine (SVM), extreme gradient boosting (XGBoost), random forest (RF), and C4.5 decision tree models are used in the literature, the absence of any study comparing these models is a gap in the literature. In this context, the performance and validation of six models in landslide susceptibility modelling are compared in this study. It is known that the northern part of Türkiye, especially the Black Sea region, has been severely affected by landslides for a long time due to excessive rainfall and is the most landslide-prone region of the country. According to Disaster and Emergency Management Presidency (AFAD), considering the number of landslide disaster cases, Rize province has the second highest number of cases after neighbouring Trabzon. In this context, Rize, the province with the highest number of landslides, was selected as the study area. Thirteen conditioning factors were considered: elevation, slope, aspect, topographic wetness index (TWI), plan curvature, profile curvature, lithology, land use, NDVI, roads, soil type, streams, and drainage density. The receiver operating characteristics (ROC), sensitivity, specificity, F-measure, accuracy, and kappa index were used for calculating the accuracy and validating the models.

MATERIALS AND METHODS

Study area

Rize, the province with the most landslides in Türkiye, is located on the eastern Black Sea coastline between 40° 30′ and 41° 20′ N and 40° 20′ and 41° 25′ E (Fig. 1). The province, which is adjacent to Trabzon in the west, Erzurum in the south, and Artvin in the east, is bordered by the Black Sea in the north. Approximately 78% of the province's territory, which totals approximately 3900 km^2, is mountainous. The average annual total precipitation is 2297.0 mm, making Rize the rainiest province in Türkiye.

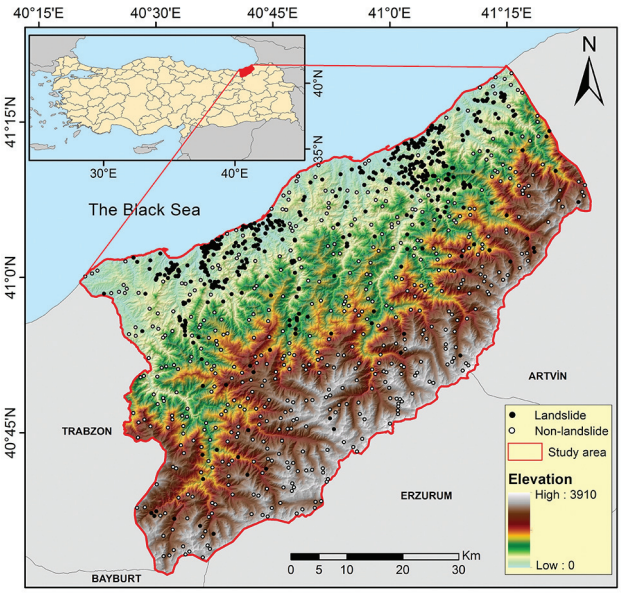

Fig. 1 Study area

Landslide conditioning factors

Thirteen conditioning factors, namely elevation, slope, aspect, topographic wetness index (TWI), plan curvature, profile curvature, lithology, land use, NDVI, roads, soil type, streams, and drainage density

were selected for landslide susceptibility mapping, considering the landslide characteristics of the study area and previous studies. Data type and sources of the factor are shown in Table 1.

The spatial relation calculated by the frequency ratio (FR) between these factors and landslide is shown in Table 2.

Landslide inventory

It is assumed that future landslides may occur in conditions similar to those that have occurred in the past (Varnes 1984). Therefore, the first and most crucial step in landslide susceptibility, hazard, or risk assessment studies is to obtain landslide inventory data.

Table 1 Data types and sources

Factor	Scale/Resolution	Data Type	Source
Elevation	12.5 m	Raster	ALOS- PALSAR digital elevation model
Slope			
TWI			
Aspect			
Plan Curvature			
Profile Curvature			
Drainage density			
Lithology	1/100000	Vector	General Directorate of Mineral Research and Exploration
Land Use	100 m	Raster	Coordination of Information on the Environment (CORINE), 2018
NDWI	30 m	Raster	The United States Geological Survey (USGS) Landsat 8 satellite image
Soil depth	1/100000	Vector	RTMAF (1991; https://tad.tarim.gov.tr/TadPortal/)
Distance to river	1/100000	Vector	Environmental Plan, Ministry of Environment and Urbanization (MEU), 2021
Distance to road			

Table 2 Frequency ratio

Factors	Classes	% of class area	% of landslide area	FR
Elevation	0–500	0.21	0.59	2.77
	500–1000	0.17	0.20	1.17
	1000–2000	0.27	0.15	0.56
	2000–3000	0.30	0.04	0.14
	3000–4000	0.04	0.02	0.37
Slope	0–10	0.41	0.16	0.38
	10–20	0.18	0.13	0.73
	20–30	0.02	0.03	1.23
	30–40	0.04	0.14	3.25
	40–50	0.08	0.26	3.29
	50–60	0.12	0.16	1.33
	>60	0.15	0.14	0.88
TWI	-1.821–3.152	0.35	0.27	0.76
	3.152–4.655	0.17	0.16	0.94
	4.655–6.043	0.41	0.45	1.09
	6.043–7.777	0.05	0.11	2.48
	7.777–10.321	0.01	0.01	0.89
	10.321–27.552	0.01	0.00	0.00
Aspect	Flat (-1)	0.01	0.00	0.00
	North (0–22.5) + (337.5–360)	0.15	0.15	1.01
	Northeast (22.5–67.5)	0.13	0.13	0.95
	East (67.5–112.5)	0.11	0.07	0.63
	Southeast (112.5–157.5)	0.08	0.10	1.20
	South (157.5–202.5)	0.10	0.11	1.17
	Southwest (202.5–247.5)	0.12	0.13	1.03
	West (247.5–292.5)	0.14	0.18	1.29
	Northwest (292.5–337.5)	0.15	0.13	0.85
Plan Curvature	-15.09–-1.82	0.03	0.03	0.98
	-1.82–-0.61	0.14	0.11	0.75
	-0.61–0.30	0.50	0.61	1.21
	0.30–1.35	0.27	0.22	0.80
	1.35–23.38	0.05	0.04	0.69

Factors	Classes	% of class area	% of landslide area	FR
Profile Curvature	-19.30 - -1.55	0.04	0.03	0.73
	-1.55–-0.44	0.22	0.20	0.91
	-0.44–0.39	0.46	0.62	1.34
	0.39–1.364	0.24	0.14	0.57
	1.64–16.06	0.04	0.02	0.44
Lithology	Alluvium	0.01	0.01	0.90
	Instrusive rocks	0.44	0.13	0.29
	Dasite riodasite and pyroclastics	0.09	0.25	2.74
	Plio-quaternary units	0.01	0.00	0.33
	Andasite basalt and pyroclastics	0.43	0.53	1.23
	Sedimantery units	0.02	0.08	4.05
Land Use	Scrub and/or herbaceous vegetation associations	0.23	0.07	0.33
	Artificial, non-agricultural vegetated areas	0.02	0.00	0.00
	Industrial, commercial and transport units	0.01	0.02	2.20
	Open spaces with little or no vegetation	0.04	0.02	0.45
	Heterogeneous agricultural areas	0.05	0.21	4.14
	Permanent crops	0.10	0.43	4.27
	Inland waters	0.01	0.01	1.09
	Urban fabric	0.25	0.00	0.00
	Pastures	0.05	0.00	0.00
	Forests	0.24	0.24	1.01
NDWI	-0.99–0.19	0.05	0.04	0.83
	0.19–0.39	0.10	0.05	0.55
	0.39–0.55	0.19	0.04	0.23
	0.55–0.67	0.26	0.23	0.88
	0.67–0.96	0.40	0.63	1.57
Soil depth	Deep	0.14	0.41	2.85
	Moderate	0.33	0.40	1.21
	Shallow	0.02	0.01	0.40
	Lithosol	0.51	0.18	0.36
Drainage density	0–0.87	0.27	0.16	0.58
	0.87–1.29	0.16	0.15	0.94
	1.29–1.76	0.05	0.05	1.01
	1.76–2.49	0.37	0.43	1.17
	2.49–3.63	0.16	0.21	1.35
Distance to river	0–250	0.09	0.13	1.33
	250–500	0.09	0.12	1.30
	500–750	0.11	0.11	1.01
	750–1000	0.10	0.11	1.08
	>1000	0.61	0.54	0.89
Distance to road	0–250	0.38	0.50	1.33
	250–500	0.17	0.20	1.13
	500–750	0.11	0.10	0.90
	750–1000	0.08	0.05	0.62
	>1000	0.25	0.15	0.58

Within the scope of this study, 204 events are from the landslide data registered in the Disaster and Emergency Management Presidency (AFAD) covering the period from 01.01.1950 to 01.10.2021, 78 events are taken from orthophoto images of the region, 147 are from previous studies, and 87 are from field studies. In total, 516 landslide inventory data were collected, and a map was created (Fig. 1).

Elevation

The elevation change can affect natural and unnatural factors, such as vegetation types and precipitation. For this reason, the height parameter has been used in many studies because it directly affects landslide susceptibility (Ali *et al.* 2021; Bui *et al.* 2020; Chang *et al.* 2019; Colkesen *et al.* 2016). A high-res-

olution (12.5 m) and radiometrically terrain corrected ALOS PALSAR digital elevation model (DEM) data was used to create an elevation map, which was divided into five classes (Fig. 2a).

Slope

Since the slope is an essential indicator in explaining the topographic structure and morphological elements of the terrain, the slope criterion is one of the most frequently used factors in landslide susceptibility analysis. In addition, the change in the slope and the deterioration of the balance of the material on the slope are the most important factors in the occurrence of the landslide (Fang *et al.* 2020; Huang, Cao *et al.* 2020; Orhan *et al.* 2022). The slope map was created using DEM data and separated into seven classes within the study area (Fig. 2b).

Aspect

The aspect, the orientation of a slope face in degrees from north, controls the decomposition rate of natural environmental features in the region, such as humidity, precipitation, wind, and sunshine duration. Therefore, soil moisture and saturation indirectly affect the factors that cause landslides, such as vegetation and soil thickness. In this context, the aspect is another parameter commonly used in landslide susceptibility studies (Huang, Chen *et al.* 2020; Kadavi *et al.* 2018; Merghadi *et al.* 2018). In this study, an aspect map is created from the DEM and is grouped into nine groups (Fig. 2c).

Topographic wetness index (TWI)

The topographic wetness index (TWI), developed by Beven, Kirkby (2009), is a parameter used in analyses to determine the potential saturation of soils or, in other words, the water-holding capacity of the surface due to the slope, and it is used very frequently in landslide studies (Mandal *et al.* 2021; Wang *et al.* 2020; Zhou *et al.* 2018). The TWI map was created using the DEM data and divided into five classes using the natural break method (Fig. 2d).

Plan curvature and profile curvature

The curvature parameter is typically determined by taking the second derivative of the line formed from the intersection of the land surface and a plane (Wilson, Gallant 2000). According to another classification system, the curvature can mostly be divided into two subclasses: profile and plan. Plan curvature is defined as a curvature determined perpendicular to the slope orientation, while profile curvature is defined as a curvature that developed parallel to the slope orientation (Olaya 2009). Many studies have emphasized that different slope curvatures have different susceptibilities to landslides (Arabameri *et al.* 2020; Chang *et al.* 2019; Hu *et al.* 2021; Huang *et al.* 2022). The plan curvature and profile curvature maps were created using DEM data and divided into five classes using the natural break method (Figs 2 e, f).

Lithology

Lithology describes the physical characteristics of rock units in the field, such as colour, texture, and grain size (Dai *et al.* 2002). In addition, different lithological formations have various shear stresses, water transmission patterns, and other susceptibility properties. Therefore, lithology has frequently been used in landslide susceptibility studies (Rane, Vincent 2022; Saha, Roy, Hembram *et al.* 2021; Yalcin 2008; Yong *et al.* 2022; Zhou *et al.* 2018).

Rize is located on the eastern Black Sea magmatic belt. This belt is of Upper Cretaceous age and consists of volcanic rocks and granitic plutons developed in Palaeozoic and Mesozoic units starting from Bulgaria and extending to Georgia. While Upper Cretaceous–Eocene magmatic rocks are observed in large parts of Rize province, Neogene sediments are also observed along the Black Sea coast. The northern areas consist of Upper Cretaceous aged tuffs and lavas, accompanied by pyroclastic flow units and volcanogenic clasts. Over these Cretaceous units, Eocene sediments and volcanics also outcrop from place to place. In the Upper Cretaceous–Eocene period, when the volcanic activity stopped, a limestone-marl-claystone and sandstone alternation is seen in a precipitated carbonate succession. At the end of the Eocene, pyroclastic units again dominated. This Cretaceous–Eocene sequence underwent a severe alteration due to the rainy climate and was covered by a clay-dominated regolith that developed due to this alteration. The region contains alternating sandstone, sandy limestone, and marl, starting with conglomerates derived from the underlying volcanic rocks during the Neogene period. The youngest deposits known in the region consist of Plio-Quaternary loose cementitious conglomerates. The pebbles belonging to all old rock units, mainly the volcanic, were formed in a completely terrestrial environment and are overlain by terraces and alluvium. From the coastline to the south and in the high mountainous area, granitic rocks and accompanying hypabyssal lavas dominate. Alluviums are encountered in parts of the great river valleys up to 10 km from the sea. The lithology map was digitized from a 1/100,000 geological map produced by the General Directorate of Mineral Research and Exploration and is shown in Fig. 3 (MTA 2005).

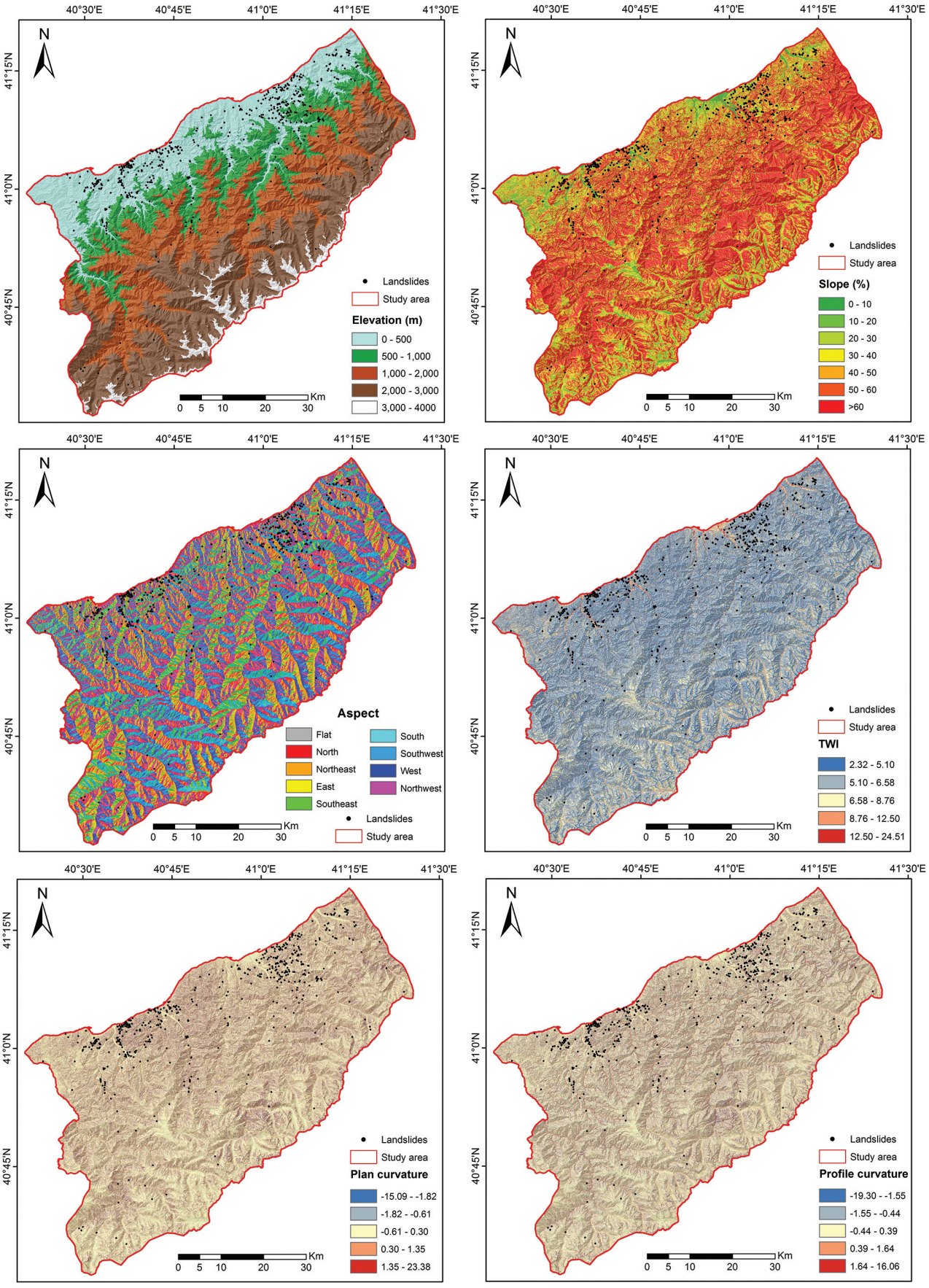

Fig. 2 a) Elevation, b) slope, c) aspect, d) topographic wetness index (TWI), e) plan curvature, and f) profile curvature map

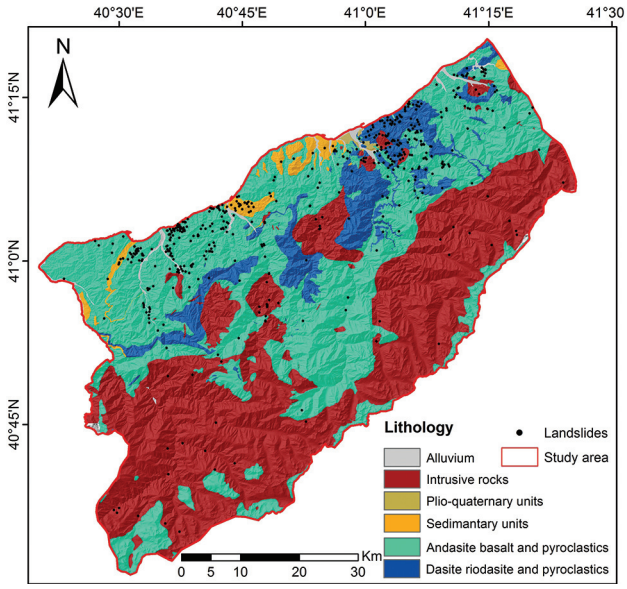

Fig. 3 Lithology map

Land use

Parameters such as land use (e.g., residential, agricultural, forested, or densely and sparsely vegetated) do not cause landslides. However, many studies evaluating landslide susceptibility have emphasized that these parameters can affect resistance to landslide formation (Ali *et al.* 2021; Hussain *et al.* 2022; Kavzoglu, Colkesen 2009; Kong *et al.* 2021). In this study, the CORINE-2018 land cover/use data was used to create a land use map, and the study area was divided into ten classes (Fig. 4a).

Normalized difference vegetation index (NDVI)

The normalized difference vegetation index (NDVI) is a parameter indicating the plant density status of the land in landslide susceptibility assess-

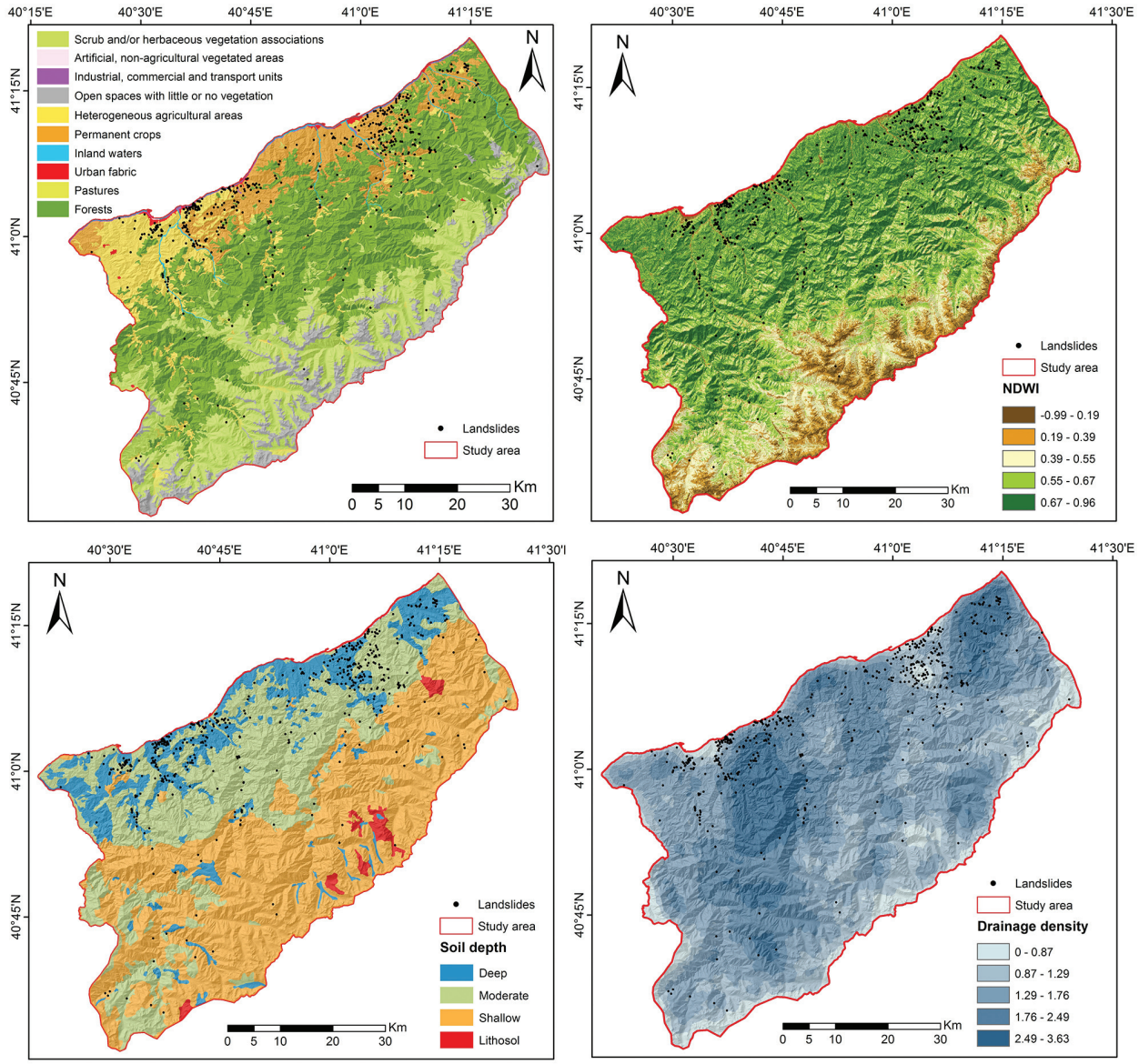

Fig. 4 a) Land use, b) normalized difference vegetation index (NDVI), c) soil depth, and d) drainage density maps

ments. NDVI is obtained by calculating the proportions of the near-infrared and red spectral ranges, to which plants are sensitive, in satellite images (Chen *et al.* 2017; He *et al.* 2012; Huang, Cao *et al.* 2020; Hussain *et al.* 2022; Youssef, Pourghasemi 2021). The NDVI map was created using Landsat 8 data for this study (Fig. 4b).

Soil depth

The landslide volume is directly related to the soil depth, which significantly affects the shear strength and stretching of the slope. It is thought that the deeper the soil, the larger the moving mass will be (Pradhan, Kim 2014). The soil map in this work was digitized from a regional soil map (1/100,000) and divided into four classes, such as deep, moderate, shallow, and lithosol (Fig. 4c).

Drainage density

Another important factor affecting stability is the drainage density, which is the ratio of the total length of the river to the basin. Areas with a high drainage density are where soil moisture is relatively high compared to drier areas, and landslides are more likely to occur (Kavzoglu *et al.* 2014; Pradhan, Kim 2014). The drainage density map was created using DEM data and divided into five classes using the natural break method (Fig. 4d).

Distance to river

The distance of the slopes to the drainage networks, such as streams and runoff channels, is one of the most important factors affecting the stability of the slopes. Streams erode the slopes and esplanades and impair their stability. In addition, streams affect the materials that make up the slopes by saturating them with water, disrupting their stability. As a result, landslides are more likely to occur in areas close to streams, where the amount of water retained in the soil will be higher than in other areas (Chen, Panahi *et al.* 2019; Pourghasemi *et al.* 2012; Pradhan *et al.* 2014). In this study, the map of the distance to a river was divided into five buffer zones (Fig. 5a).

Distance to roads

Topography is constantly changing due to various development activities. Particularly in mountainous regions, the construction of road networks by cutting into the slopes is vital and makes these regions vulnerable to slope slides. For this reason, many studies have emphasized the importance of the distance to the road parameter (Bai *et al.* 2021; Chen *et al.* 2017, 2019a; Hong *et al.* 2019; Kidanu *et al.* 2018; Reis *et al.* 2012). Similar to the effect of the distance to rivers, landslides may occur on the road and the side of the slopes affected by roads (Yalcin 2008). In this study, the distance to road maps was divided into five zones (Fig. 5b).

Machine learning models

Naive Bayes (NB)

The NB algorithm, a fast learner classification technique frequently used in many earth science applications, is suitable for classification in large-scale, mixed, and incomplete datasets (Ali *et al.* 2021; Chen *et al.* 2019b; Pham, Shirzadi *et al.* 2018; Taheri *et al.* 2019). Furthermore, using NB raises the prob-

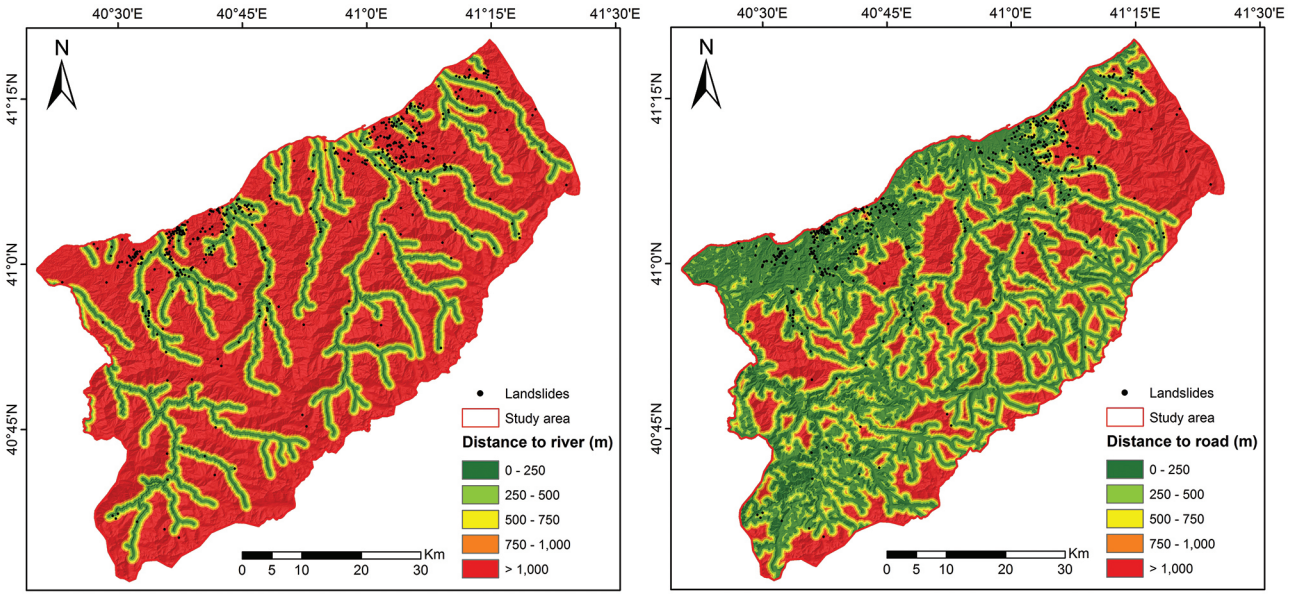

Fig. 5 a) Distance to river and b) distance to road maps

ability of classification in cases without dependency between the variables and the conditioning factors. In landslide susceptibility modelling, the NB algorithm has four main steps: first, the training dataset is selected; second, the posterior probability of each class is determined; third, class level and covariance matrix are calculated; and finally, a discriminant function for separate classes is created (i.e., landslide/non-landslide classes) (Ali *et al.* 2021; Khosravi *et al.* 2016)

C4.5 decision tree

The C4.5 decision tree (C4.5) is a decision tree algorithm developed from the ID3 algorithm derived from information theory and is widely used in classification problems (Bui *et al.* 2020). C4.5 can deal with continuous dependent variables without branch limitations and uses entropy and information gain criteria to select the best dividing feature. In the C4.5 algorithm, when all samples belong to the same class, a leaf node is created, and this node is given the name of this class. If none of the features have information gain and an unprecedented class emerges, it creates a decision node using the expected value of the class (Hu *et al.* 2021).

Random Forest

Random forest (RF) is an ensemble approach that uses decision tree models widely used for classification and regression problems and was generated by Breiman (2001). The RF model branches all the nodes by choosing the best randomly picked attributes in each node instead of branching the nodes selected from the best attributes in the dataset. Each dataset is generated by displacement from the original dataset (Akinci, Zeybek 2021; Iban, Sekertekin 2022; Merghadi *et al.* 2020; Orhan *et al.* 2022; Rane, Vincent 2022; Wang *et al.* 2020).

Extreme gradient boosting (XGBoost)

XGBoost has been widely used for classification and regression problems in many geoscience applications (Aydin, Iban 2022; Hussain *et al.* 2022; Iban, Bilgilioglu 2023; Shmuel, Heifetz 2022). XGBoost constantly produces new trees by correcting the error of previous trees, which is the most significant difference from the RF method. The number of trees and the learning rate are the main parameters of the XGBoost model because XGBoost aims to enhance the output of multiple imperfect learners by merging them (Hussain *et al.* 2022).

Support vector machine (SVM)

The SVM model is a supervised machine learning model based on statistical learning theory, which has been widely used for classification and regression problems and was developed by Vapnik (1995). The main principle of the model is structural risk minimization. The main characteristic of SVM models is that during the learning process, the initial input space is transformed into a higher-dimensional feature space to estimate an ideal separating hyperplane and classify new unknown examples into known classes (Akinci, Zeybek 2021; Chang *et al.* 2019; Huang, Chen *et al.* 2020; Kong *et al.* 2021; Pham, Prakash *et al.* 2018).

Artificial neural network (ANN)

ANN is a computational program modelled on the neural network of the human brain that has been widely used in landslide susceptibility modelling (Al-Najjar, Pradhan 2021; Bragagnolo *et al.* 2020; Hu *et al.* 2021; Saha, Roy, Hembram *et al.* 2021; Xie *et al.* 2021; Youssef, Pourghasemi 2021; Zhou *et al.* 2018). ANN aims to develop a model for forecasting the output of input factors. The multi-layer perceptron (MLP) consists of three layers: input, hidden, and output, which is the typical network structure. In addition, the backpropagation neural network (BPNN) is one of the most influential ANNs in LSM. In the training stage, the BPNN model chooses the weight of the input layers, and the mean-square error is calculated to find the differences between the calculated and the expected values for all layers. The generalized delta rule updates each weight in the backpropagation stage. This procedure occurs iteratively until the error of the network reaches an adequate value (Orhan *et al.* 2022).

Preparation of training and validation datasets

In order to create landslide susceptibility models, two clusters, landslide and non-landslide, should be created. In this context, in addition to the inventory data (positive) of up to 516 data points, the same number of non-landslide (negative) samples were randomly selected. In addition, the data to be used to create the model and validation should be divided at a certain rate. Although the literature does not show a consistent ratio, a ratio of 70:30 was used in this study, in agreement with many other studies. In this context, 1032 landslide and non-landslide samples were randomly divided. Accordingly, up to 722 (70%) points were used for training and 310 (30%) for verification.

Model performance and validation methods

It is very important to evaluate the performance of a model created with ML. There is no value or meaning in building a model without validation. However, there is no clear consensus on which method should be used to evaluate performance and accuracy in ML

Table 3 Statistical measurements

Statistical methods	Formula	Description
Sensitivity	$\frac{TP}{FN + TP}$	The ability to find landslide samples.
Specificity	$\frac{TP}{FB + TN}$	The ability to find non-landslide samples.
Accuracy	$\frac{TP + TN}{TP + FN + FP + TN}$	Overall accuracy of classification.
AUC	$\frac{1}{2}\left(\frac{TN}{TN + FN} + \frac{TP}{TP + FN}\right)$	The ability of a classifier to avoid mis-classification.
Kappa	$\frac{Accuracy - Px}{1 - Px}$ where: $Px = \frac{(TN + FP) \times (TN + FN) \times (FN + TP) \times (FP + TP)}{(TN + TP + FN + FP)^2}$	Agreement between the model and reality.

studies. Various metrics are used to evaluate model performance and accuracy. The model performance metrics used in the study are presented in Table 3. True Positives (TP) describes the number of samples that are landslides in the dataset and classified as landslides by the model. True Negatives (TN) describes the number of samples that are non-landslides in the dataset and are classified as non-landslides by the model. The number of samples classified as non-landslide samples by the model but identified as landslides in the dataset is known as False Positives (FP), while the number of samples classified as landslides by the model but identified as non-landslide samples in the dataset is known as False Negatives (FN). The calculation of these metrics requires the use of an error matrix, which forms the basis for auditing the model performance (Colkesen *et al.* 2016; Huang, Cao *et al.* 2020; Huang, Chen *et al*. 2020; Kadavi *et al.* 2018; Pradhan *et al.* 2014). Specificity, accuracy, and kappa (κ) index were calculated for each model run using TP, FN, TN and FP values. Other metrics used is Area Under the Curve (AUC). Receiver operator characteristic (ROC) curves can be used as a performance evaluation metric for binary classification tasks using a probability curve. The ROC curve is a useful tool for evaluating the results of predictions. A ROC curve is a curve in which the rates of true positivity (sensitivity) on the vertical axis and false positivity (1−specificity) on the horizontal axis are shown for different threshold values. Each point on the ROC curve reveals the sensitivity and 1−specificity values corresponding to different threshold values. Threshold values that generally give low false positive rates also have low true positive rates. As the true positivity rate increases, the false positivity rate also increases. The area under the ROC is between 0.50 and 1.00, depending on the activity level. The higher the AUC, the better the classification performance. An AUC higher than 0.9 indicates that the classification is almost perfect (Colkesen *et al.* 2016; He *et al.* 2012; Kong *et al.* 2021; Kutlug Sahin, Colkesen 2021; Oh *et al.* 2019; Pradhan *et al.* 2014; Sarkar *et al.* 2013).

RESULTS

LSM conditioning factor analysis

In machine learning studies, it is crucial to evaluate the appropriateness of the chosen factors before the model training stage. In this research, the Relief F feature selection method, developed by Kira, Rendell (1992) and frequently employed in landslide susceptibility studies, was utilized to assess the impact of the 13 selected factors on the model. The Relief F method relies on probability theory and determines the effect of the selected factor based on their conditional dependencies. In this regard, it computes factor weights to evaluate the significance and suitability of factors. A higher weight value indicates a greater influence of the factor. On the other hand, a lower weight signifies a lesser impact, and if the weight is "0," the criterion has no effect on the model and should not be included since it is irrelevant to the current analysis. In this study, the average merit (AM) values of all factors are presented in Table 4. As all 13 factors had values greater than zero, they were all incorporated into the model training process. Furthermore, as depicted in Table 4, the distance to road had the highest predictive capability with the highest AM value of 0.0821, followed by lithology (AM: 0.0781), drainage density (AM: 0.0734), while the factors with the least effect are elevation (AM: 0.0405), aspect (0.0371), and profile curvature (0.0311).

Model construction

In a previous study, six machine learning models were built using the tenfold cross-validation approach with a training dataset. For each of the six models, Landslide Susceptibility Indices (LSI) were generated and subsequently reclassified into five categories (very low, low, moderate, high, and very high susceptibility). In the literature, there are different methods used to reclassify the generated index map, such as equal interval, quantile, standard deviation, natural

Table 4 Average merit (AM) values of the landslide conditioning factors

Landslide conditioning factors	Average merit (AM)	Standard deviation (Sd)
Distance to roads	0.0821	0.005
Lithology	0.0781	0.004
Drainage density	0.0734	0.006
Slope	0.0711	0.007
TWI	0.0694	0.010
Soil depth	0.0657	0.004
Distance to rivers	0.0601	0.009
Land use	0.0574	0.011
NDVI	0.0501	0.007
Plan curvature	0.0497	0.008
Elevation	0.0405	0.011
Aspect	0.0371	0.008
Profile curvature	0.0311	0.010

Table 5 Areal dis1tribution of each susceptibility class

Susceptibility class	XGBoost (%)	RF (%)	ANN (%)	SVM (%)	C4.5 (%)	NB (%)
Very low	3.14	3.25	2.74	2.94	2.56	3.21
Low	9.58	15.58	7.22	16.05	10.07	15.53
Moderate	28.93	26.50	29.09	25.54	28.72	31.39
High	28.22	30.54	33.50	32.76	37.02	32.23
Very high	30.14	24.14	27.46	22.72	21.62	17.64

Table 6 Parameters of the AUC (training sample)

Model	AUC	Std. Error		Confidence interval (95%)		
				Lower Bound	Upper Bound	Significance level (Area = 0.05)
XGBoost	0.941	0.0211	0.030	0.911	0.971	0.0001
RF	0.934	0.0234	0.034	0.900	0.968	0.0001
ANN	0.927	0.0239	0.040	0.887	0.967	0.0001
SVM	0.911	0.0244	0.042	0.869	0.953	0.0001
C4.5	0.893	0.0258	0.044	0.849	0.937	0.0001
NB	0.871	0.0279	0.048	0.823	0.919	0.0001

break, and geometric interval. The histogram of the index map was analyzed and the best classification result was obtained with the natural break method. In this context, the intervals for the indices were determined using the natural break method, resulting in the creation of landslide susceptibility maps (Fig. 6).

Figure 6 displays the spatial distribution of each susceptibility class as a percentage and the proportion of landslide samples that correspond to these risk classes. The XGBoost model estimates that 30.14% of the study area exhibits very high susceptibility, 28.22% high, 28.93% moderate, 9.58% low, and 3.14% very low susceptibility. In the LSM produced by the RF model, 24.14% of the study area is classified as having very high susceptibility, 30.54% high, 26.50% moderate, 15.58% low, and 3.25% very low susceptibility. According to the ANN model, 27.46% of the study area has very high susceptibility, while 33.50%, 29.09%, 7.22%, and 2.74% of the study area fall under the high, moderate, low, and very low susceptibility categories, respectively. The SVM model predicts that 22.72% of the study area has very high susceptibility, 32.76% high, 25.54% moderate, 16.05% low, and 2.94% very low susceptibility. Regarding the LSM developed by the C4.5 model, 21.62% of the study area displays very high susceptibility, while 37.02%, 28.72%, 10.07%, and 2.56% of the study area are identified as having high, moderate, low, and very low susceptibility, respectively. The NB model estimates that 17.64% of the study area has very high susceptibility, 32.23% high, 31.39% moderate, 15.53% low, and 3.21% very low susceptibility (Table 5).

Model performance and validation

The performance of the six ML models was measured using ROC and statistical methods such as sensitivity, specificity, accuracy, and the kappa index. The XGBoost model had the highest AUC value (0.941), followed by the RF model (0.934), ANN model (0.927), SVM model (0.911), C4.5 model (0.893), and NB model (0.871). The results are summarized in Table 6.

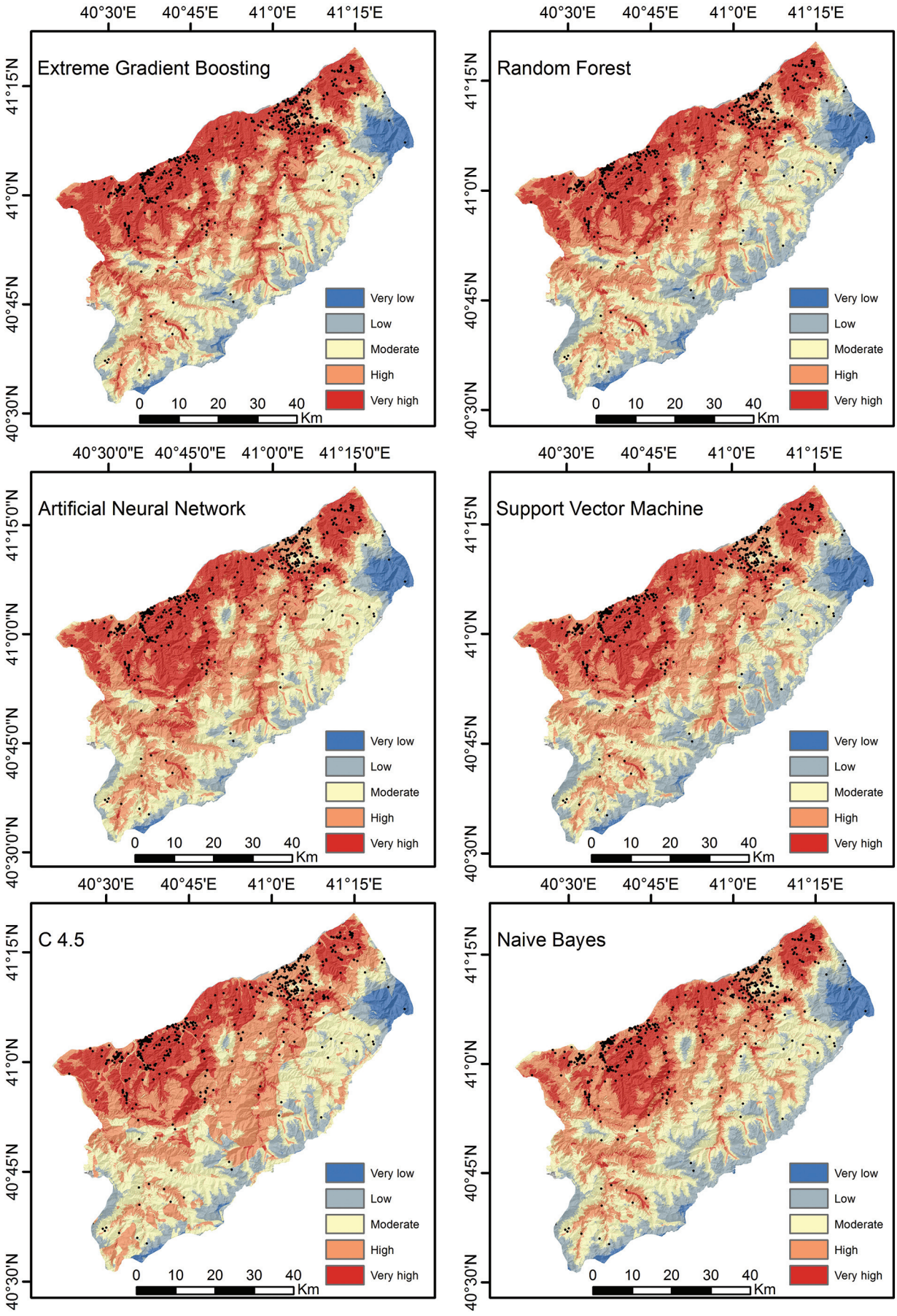

Fig. 6 Landslide susceptibility maps (a: XGBoost, b: RF, c: ANN, d: SVM, e: C4.5, and f: NB)

Table 7 reveals that the XGBoost model achieved the best landslide pixel classification performance (sensitivity) at 93.92%, followed by the RF model (93.09%), ANN model (92.52%), SVM model (91.67%), C4.5 model (90.00%), and NB model (87.50%). The XGBoost model also exhibited the highest performance in classifying non-landslide pixels (specificity) at 94.17%, followed by the RF model (93.33%), ANN model (92.52%), SVM model (91.44%), C4.5 model (89.78%), and NB model (87.29%). In terms of accuracy, the XGBoost model ranked highest with 94.04%, followed by the RF model (93.21%), ANN model (92.52%), SVM model (91.55%), C4.5 model (89.89%), and NB model (87.40%). The kappa index for all six models ranged from 74.79% to 88.09%, demonstrating sufficient agreement between the models and actual conditions.

The ROC curve was used to evaluate the prediction probability of the models with validation dataset (Table 8). The XGBoost model had the highest prediction probability with the highest AUC value (0.923), followed by the RF model (0.918), ANN model (0.907), SVM model (0.891), C4.5 model (0.877), and NB model (0.858).

Furthermore, a variety of statistical index-based assessments were employed to gauge the performance of the six models, as detailed in Table 9. The XGBoost model achieved the highest performance in landslide pixel classification (92.31%), followed by the RF model (91.61%), ANN model (90.91%), SVM model (89.68%), C4.5 model (88.89%), and NB model (85.71%). For non-landslide pixel classification, the XGBoost model demonstrated the highest performance (specificity = 92.86%), followed by the RF model (91.61%), ANN model (90.38%), SVM model (89.68%), C4.5 model (97.90%), and NB model (85.48%). In terms of accuracy, the XGBoost model exhibited the highest value at 92.58%, with the RF model (91.61%), ANN model (90.65%), SVM model (89.68%), C4.5 model (88.39%), and NB model (85.48%) following suit. The kappa index for all models fell between 70.97% and 85.16%, indicating an adequate level of agreement between these models and the actual situation.

Overall, comparing all six models with the training and validation datasets shows acceptable goodness of fit. One of these six models, the XGBoost model, gave better results than the other five models.

Table 7 Model performance

	XGBoost	RF	ANN	SVM	C4.5	NB
TP	340	337	334	330	324	315
TN	339	336	334	331	325	316
FP	21	24	27	31	37	46
FN	22	25	27	30	36	45
Sensitivity	93.92%	93.09%	92.52%	91.67%	90.00%	87.50%
Specificity	94.17%	93.33%	92.52%	91.44%	89.78%	87.29%
Accuracy	94.04%	93.21%	92.52%	91.55%	89.89%	87.40%
Kappa Index	88.09%	86.43%	85.04%	83.10%	79.78%	74.79%

Table 8 Parameters of the AUC (test sample)

Model	AUC	Std. Error		Confidence interval (95%)		
				Lower Bound	Upper Bound	Significance level (Area = 0.05)
XGBoost	0.923	0.941	0.034	0.889	0.957	0.0001
RF	0.918	0.934	0.041	0.877	0.959	0.0001
ANN	0.907	0.927	0.042	0.865	0.949	0.0001
SVM	0.891	0.911	0.045	0.846	0.936	0.0001
C4.5	0.877	0.893	0.047	0.830	0.924	0.0001
NB	0.858	0.871	0.05	0.808	0.908	0.0001

Table 9 Model validation

	XGBoost	RF	ANN	SVM	C4.5	NB
TP	144	142	140	139	136	132
TN	143	142	141	139	138	133
FP	11	13	15	16	19	23
FN	12	13	14	16	17	22
Sensitivity	92.31%	91.61%	90.91%	89.68%	88.89%	85.71%
Specificity	92.86%	91.61%	90.38%	89.68%	87.90%	85.26%
Accuracy	92.58%	91.61%	90.65%	89.68%	88.39%	85.48%
Kappa Index	85.16%	83.23%	81.29%	79.35%	76.77%	70.97%

DISCUSSION

In this study, six different machine learning models (XGBoost, RF, ANN, SVM, C4.5, and NB) have been employed to create a landslide susceptibility map for the Rize province. The performance of the models was assessed using the ROC curve and statistical values (sensitivity, specificity, accuracy, and kappa index). The results indicate that the XGBoost model outperforms other machine learning models in terms of accuracy and performance, making it the most effective model for creating landslide susceptibility maps.

Upon examining the performance of the models, it is observed that some models produce better results for the specific factor compared to others. The XGBoost model exhibits the highest Area Under the Curve (AUC) value (0.941) and demonstrates the best results compared to other models. A high performance of this model is attributed to its ability to capture complex nonlinear relationships between features. Additionally, the XGBoost model presents the highest accuracy, sensitivity, and specificity rates according to the ROC curve and other statistical evaluations. Other models, such as random forest, artificial neural network, and support vector machine, also demonstrate good performance. In particular, the RF model attracts attention with an AUC value (0.934) and accuracy rate close to the XGBoost model. While ANN and SVM models provide lower accuracy and sensitivity rates, they still offer sufficient information. The C4.5 decision tree and naive Bayes models exhibit lower performance compared to other models, with lower AUC values and accuracy rates. However, it should not be overlooked that these models may be preferred due to their simpler structures and lower computational requirements. One of the reasons for a higher accuracy rate of the XGBoost model is the application of methods that prevent overfitting and promote regularization, which reduce the model's complexity and increase its generalization ability. Moreover, XGBoost employs gradient boosting techniques that iteratively correct errors in decision trees, enhancing the model's performance.

The average merit values of landslide conditioning factors play a significant role in the analysis of this study. These values help illustrate the impact of each factor on landslide susceptibility and can be used as an additional criterion for evaluating model performance. Factors with high average merit values should be considered as the most influential factors affecting model performance.

In a previous study conducted by Reis *et al*. (2012), the frequency ratio and Analytical Hierarchy Process (AHP) methods were used to create a landslide susceptibility map for the Rize province. Compared to this study, machine learning models provide results with higher accuracy. These models, especially XGBoost, offer higher accuracy rates and performance compared to the methods employed in previous studies. Therefore, in regions with a high landslide risk such as Rize, the use of machine learning models is an essential tool for creating more accurate and reliable landslide susceptibility maps. Machine learning models such as XGBoost, known for their remarkable accuracy, play an important role in assisting local and regional governments, urban planners and engineers in mitigating landslide risk, developing infrastructure initiatives and formulating policies related to natural disasters. Although these models were developed in this study based on data from Rize province, their adaptability to different and new datasets makes them applicable in various regions. This research provides a remarkable example of comparing ML models in the creation of landslide susceptibility maps on an important dataset. The excellent performance of these ML models on the large dataset used in this study constitutes an important contribution to the literature on landslide susceptibility research. However, even with the use of high-performance computing resources, some ML models face limitations when dealing with extensive datasets within a reasonable time frame. While the results of this study highlight the effectiveness of five different machine learning models in assessing landslide susceptibility, further research using different datasets is necessary to validate these findings. Moreover, it is crucial to benchmark these models against alternative ML techniques to establish the most suitable one.

CONCLUSION

This study compared six different ML models (XGBoost, RF, ANN, SVM, C4.5, and NB), for which performance and validation comparisons have not previously been performed in landslide susceptibility modelling studies. A total of 13 conditioning factors were selected to create the landslide susceptibility models. These factors are: distance to roads, lithology, drainage density, slope, TWI, soil depth, distance to rivers, land use, NDVI, plan curvature, elevation, aspect, and profile curvature. The effects of these factors on the model were calculated using the ReliefF method, and it was determined that all factors influenced the model. The performance and validation of the models were compared with the ROC curve and various other statistical methods. As a result of the comparison, the performance and prediction capabilities of all models are acceptable. Because of its better performance and validation results, the XGBoost model is superior to the other five models. Comparing these and similar ML models is essen-

tial to reveal the capabilities of the models. Future research should focus on improving the accuracy and reliability of landslide susceptibility maps by further improving existing machine learning models or applying new methods and techniques. In this context, increasing the number of this type of study will benefit decision-makers making land use plans.

ACKNOWLEDGEMENT

The author is indebted to the anonymous reviewers and the editors for their valuable and constructive suggestions. In this study, there are no funding information and organization.

REFERENCES

Akinci, H., Zeybek, M. 2021. Comparing classical statistic and machine learning models in landslide susceptibility mapping in Ardanuc (Artvin), Turkey. *Natural Hazards 108*, 1515–1543. https://doi.org/10.1007/s11069-021-04743-4

Al-Najjar, H.A.H., Pradhan, B. 2021. Spatial landslide susceptibility assessment using machine learning techniques assisted by additional data created with generative adversarial networks. *Geoscience Frontiers 12*, 625–637. https://doi.org/10.1016/j.gsf.2020.09.002

Ali, S.A., Parvin, F., Vojteková, J., Costache, R., Linh, N.T.T., Pham, Q.B., Vojtek, M., Gigović, L., Ahmad, A., Ghorbani, M.A. 2021. GIS-based landslide susceptibility modelling: A comparison between fuzzy multi-criteria and machine learning algorithms. *Geoscience Frontiers 12*, 857–876. https://doi.org/10.1016/j.gsf.2020.09.004

AlSanea, D., Abdullah, W. 2021. Sinkhole Susceptibility Hazard Mapping Using Analytical Hierarchy Process and GIS Tools for the State of Kuwait. *ASCE-ASME Journal of Risk and Uncertainty in Engineering Systems, Part A: Civil Engineering 7*, 04021029. https://doi.org/10.1061/AJRUA6.0001136

Arabameri, A., Saha, S., Roy, J., Chen, W., Blaschke, T., Bui, D.T. 2020. Landslide susceptibility evaluation and management using different machine learning methods in the Gallicash River Watershed, Iran. *Remote Sensing 12*. https://doi.org/10.3390/rs12030475

Aydin, H.E., Iban, M.C. 2022. Predicting and analysing flood susceptibility using boosting-based ensemble machine learning algorithms with SHapley Additive explanations. *Natural Hazards 2022*, 1–35. https://doi.org/10.1007/S11069-022-05793-Y

Bai, Z., Liu, Q., Liu, Y. 2021. Landslide susceptibility mapping using GIS-based machine learning algorithms for the Northeast Chongqing Area, China. *Arabian Journal of Geosciences 14*. https://doi.org/10.1007/s12517-021-08871-w

Beven, K.J., Kirkby, M.J. 2009. *A physically based, variable contributing area model of basin hydrology*, 24, 43–69. https://doi.org/10.1080/02626667909491834

Bragagnolo, L., Silva, R.V. d., Grzybowski, J.M.V. 2020. Artificial neural network ensembles applied to the mapping of landslide susceptibility. *Catena 184*, 104240. https://doi.org/10.1016/J.CATENA.2019.104240

Breiman, L. 2001. Random Forests. *Machine Learning 2001 (45)*, 5–32. https://doi.org/10.1023/A:1010933404324

Bui, D.T., Tsangaratos, P., Nguyen, V.T., Liem, N. Van, Trinh, P.T. 2020. Comparing the prediction performance of a Deep Learning Neural Network model with conventional machine learning models in landslide susceptibility assessment. *Catena 188*, 104426. https://doi.org/10.1016/j.Catena.2019.104426

Chang, K.T., Merghadi, A., Yunus, A.P., Pham, B.T., Dou, J. 2019. Evaluating scale effects of topographic variables in landslide susceptibility models using GIS-based machine learning techniques. *Scientific Reports 9*, 1–21. https://doi.org/10.1038/s41598-019-48773-2

Che, V.B., Kervyn, M., Suh, C.E., Fontijn, K., Ernst, G.G.J., Del Marmol, M.A., Trefois, P., Jacobs, P. 2012. Landslide susceptibility assessment in Limbe (SW Cameroon): A field calibrated seed cell and information value method. *Catena 92*, 83–98. https://doi.org/10.1016/J.CATENA.2011.11.014

Chen, W., Pourghasemi, H.R., Panahi, M., Kornejady, A., Wang, J., Xie, X., Cao, S. 2017. Spatial prediction of landslide susceptibility using an adaptive neuro-fuzzy inference system combined with frequency ratio, generalized additive model, and support vector machine techniques. *Geomorphology 297*, 69–85. https://doi.org/10.1016/J.GEOMORPH.2017.09.007

Chen, W., Peng, J., Hong, H., Shahabi, H., Pradhan, B., Liu, J., Zhu, A.X., Pei, X., Duan, Z. 2018. Landslide susceptibility modelling using GIS-based machine learning techniques for Chongren County, Jiangxi Province, China. *Science of the Total Environment 626*, 1121–1135. https://doi.org/10.1016/j.scitotenv.2018.01.124

Chen, W., Panahi, M., Tsangaratos, P., Shahabi, H., Ilia, I., Panahi, S., Li, S., Jaafari, A., Ahmad, B. Bin. 2019a. Applying population-based evolutionary algorithms and a neuro-fuzzy system for modeling landslide susceptibility. *Catena 172*, 212–231. https://doi.org/10.1016/J.CATENA.2018.08.025

Chen, W., Yan, X., Zhao, Z., Hong, H., Bui, D.T., Pradhan, B. 2019b. Spatial prediction of landslide susceptibility using data mining-based kernel logistic regression, naive Bayes and RBFNetwork models for the Long County area (China). *Bulletin of Engineering Geology and the Environment 78*, 247–266. https://doi.org/10.1007/S10064-018-1256-Z/FIGURES/12

Colkesen, I., Sahin, E.K., Kavzoglu, T. 2016. Susceptibility mapping of shallow landslides using kernel-based Gaussian process, support vector machines and logistic regression. *Journal of African Earth Sciences 118*, 53–64. https://doi.org/10.1016/j.jafrearsci.2016.02.019

Dai, F.C., Lee, C.F., Ngai, Y.Y. 2002. Landslide risk assessment and management: an overview. *Engineering Geology 64*, 65–87. https://doi.org/10.1016/S0013-7952(01)00093-X

Ercanoglu, M., Gokceoglu, C. 2002. Assessment of landslide susceptibility for a landslide-prone area (north of Yenice, NW Turkey) by fuzzy approach. *Environmental Geology 41*, 720–730. https://doi.org/10.1007/S00254-001-0454-2

Fang, Z., Wang, Y., Peng, L., Hong, H. 2020. Integration of convolutional neural network and conventional machine learning classifiers for landslide susceptibility mapping. *Computers and Geosciences 139*, 104470. https://doi.org/10.1016/j.cageo.2020.104470

He, S., Pan, P., Dai, L., Wang, H., Liu, J. 2012. Application of kernel-based Fisher discriminant analysis to map landslide susceptibility in the Qinggan River delta, Three Gorges, China. *Geomorphology 171–172*, 30–41. https://doi.org/10.1016/J.GEOMORPH.2012.04.024

Hong, H., Shahabi, H., Shirzadi, A., Chen, W., Chapi, K., Ahmad, B. Bin, Roodposhti, M.S., Yari Hesar, A., Tian, Y., Tien Bui, D. 2019. Landslide susceptibility assessment at the Wuning area, China: a comparison between multi-criteria decision making, bivariate statistical and machine learning methods. *Natural Hazards 96,* 173–212.

Hu, X., Mei, H., Zhang, H., Li, Y., Li, M. 2021. Performance evaluation of ensemble learning techniques for landslide susceptibility mapping at the Jinping county, Southwest China. *Natural Hazards 105*, 1663–1689. https://doi.org/10.1007/s11069-020-04371-4

Huang, F., Cao, Z., Guo, J., Jiang, S.H., Li, S., Guo, Z. 2020. Comparisons of heuristic, general statistical and machine learning models for landslide susceptibility prediction and mapping. *Catena 191*, 104580. https://doi.org/10.1016/j.Catena.2020.104580

Huang, F., Chen, J., Du, Z., Yao, C., Huang, J., Jiang, Q., Huang, F., Chen, J., Du, Z., Yao, C., Huang, J., Jiang, Q., Li, S. 2020. Landslide susceptibility prediction considering regional soil erosion based on machine-learning models. *ISPRS International Journal of Geo-Information 9 (6),* 377.

Huang, F., Yan, J., Fan, X., Yao, C., Huang, J., Chen, W., Hong, H. 2022. Uncertainty pattern in landslide susceptibility prediction modelling: Effects of different landslide boundaries and spatial shape expressions. *Geoscience Frontiers 13*, 101317. https://doi.org/10.1016/j.gsf.2021.101317

Hussain, M.A., Chen, Z., Kalsoom, I., Asghar, A., Shoaib, M. 2022. Landslide Susceptibility Mapping Using Machine Learning Algorithm: A Case Study Along Karakoram Highway (KKH), Pakistan. *Journal of the Indian Society of Remote Sensing 50*, 849–866. https://doi.org/10.1007/s12524-021-01451-1

Iban, M.C., Sekertekin, A. 2022. Machine learning based wildfire susceptibility mapping using remotely sensed fire data and GIS: A case study of Adana and Mersin provinces, Turkey. *Ecological Informatics 69*, 101647. https://doi.org/10.1016/J.ECOINF.2022.101647

Iban, M.C., Bilgilioglu, S.S. 2023. Snow avalanche susceptibility mapping using novel tree-based machine learning algorithms (XGBoost, NGBoost, and LightGBM) with eXplainable Artificial Intelligence (XAI) approach. *Stochastic Environmental Research and Risk Assessment 37*, 2243–2270. https://doi.org/10.1007/S00477-023-02392-6

Kadavi, P.R., Lee, C.W., Lee, S. 2018. Application of ensemble-based machine learning models to landslide susceptibility mapping. *Remote Sensing 10*, 1–18. https://doi.org/10.3390/rs10081252

Kavzoglu, T., Colkesen, I. 2009. A kernel functions analysis for support vector machines for land cover classification. *International Journal of Applied Earth Observation and Geoinformation 11*, 352–359. https://doi.org/10.1016/J.JAG.2009.06.002

Kavzoglu, T., Sahin, E.K., Colkesen, I. 2014. Landslide susceptibility mapping using GIS-based multi-criteria decision analysis, support vector machines, and logistic regression. *Landslides 11*, 425–439. https://doi.org/10.1007/s10346-013-0391-7

Kavzoglu, T., Kutlug Sahin, E., Colkesen, I. 2015. An assessment of multivariate and bivariate approaches in landslide susceptibility mapping: a case study of Duzkoy district. *Natural Hazards 76*, 471–496. https://doi.org/10.1007/S11069-014-1506-8/TABLES/4

Khosravi, K., Nohani, E., Maroufinia, E., Pourghasemi, H.R. 2016. A GIS-based flood susceptibility assessment and its mapping in Iran: a comparison between frequency ratio and weights-of-evidence bivariate statistical models with multi-criteria decision-making technique. *Natural Hazards 83*, 947–987. https://doi.org/10.1007/S11069-016-2357-2/TABLES/9

Kidanu, S.T., Anderson, N.L., Rogers, J.D. 2018. Using Gis-based Spatial Analysis To Determine Factors Influencing the Formation of Sinkholes in Greene County, Missouri. *Environmental & Engineering Geoscience 24*, 251–261. https://doi.org/10.2113/EEG-2014

Kira, K., Rendell, L.A. 1992. A Practical Approach to Feature Selection. *Machine Learning Proceedings 1992*, 249–256. https://doi.org/10.1016/B978-1-55860-247-2.50037-1

Kong, C., Tian, Y., Ma, X., Weng, Z., Zhang, Z., Xu, K. 2021. Landslide susceptibility assessment based on different machine learning methods in Zhaoping county of eastern Guangxi. *Remote Sensing 13*. https://doi.org/10.3390/rs13183573

Kutlug Sahin, E., Colkesen, I. 2019. *Performance analysis of advanced decision tree-based ensemble learning algorithms for landslide susceptibility mapping*. 36, 1253–1275. https://doi.org/10.1080/10106049.2019.1641560

Kutlug Sahin, E., Colkesen, I. 2021. Performance analysis of advanced decision tree-based ensemble learning algorithms for landslide susceptibility mapping. *Geocarto International 36*, 1253–1275. https://doi.org/10.1080/10106049.2019.1641560

Luo, W., Liu, C.C. 2018. Innovative landslide susceptibility mapping supported by geomorphon and geographical detector methods. *Landslides 15*, 465–474. https://doi.org/10.1007/S10346-017-0893-9/TABLES/2

Mandal, K., Saha, S., Mandal, S. 2021. Applying deep learning and benchmark machine learning algorithms for landslide susceptibility modelling in Rorachu river basin of Sikkim Himalaya, India. *Geoscience Frontiers 12*, 101203. https://doi.org/10.1016/j.gsf.2021.101203

Merghadi, A., Abderrahmane, B., Tien Bui, D. 2018. Landslide susceptibility assessment at Mila basin (Algeria): A comparative assessment of prediction capability of advanced machine learning methods. *ISPRS International Journal of Geo-Information 7*. https://doi.org/10.3390/ijgi7070268

Merghadi, A., Yunus, A.P., Dou, J., Whiteley, J., Thai-Pham, B., Bui, D.T., Avtar, R., Abderrahmane, B. 2020. Machine learning methods for landslide susceptibility studies: A comparative overview of algorithm performance. *Earth-Science Reviews 207*, 103225. https://doi.org/10.1016/j.earscirev.2020.103225

MTA. 2005. 1/100 000 ölçekli Türkiye JeolojiHaritasıserisi.

Oh, H.J., Syifa, M., Lee, C.W., Lee, S. 2019. Land Subsidence Susceptibility Mapping Using Bayesian, Functional, and Meta-Ensemble Machine Learning Models. *Applied Sciences 9*, 1248–1248. https://doi.org/10.3390/APP9061248

Olaya, V. 2009. Chapter 6 Basic Land-Surface Parameters. *Developments in Soil Science 33*, 141–169. https://doi.org/10.1016/S0166-2481(08)00006-8

Orhan, O., Bilgilioglu, S.S., Kaya, Z., Ozcan, A.K., Bilgilioglu, H. 2022. Assessing and mapping landslide susceptibility using different machine learning methods. *Geocarto International 37*, 2795–2820. https://doi.org/10.1080/10106049.2020.1837258

Pham, B.T., Prakash, I., Khosravi, K., Chapi, K., Trinh, P.T., Ngo, T.Q., Hosseini, S. V., Bui, D.T. 2018. A comparison of Support Vector Machines and Bayesian algorithms for landslide susceptibility modelling. *Geocarto International 34*, 1385–1407. https://doi.org/10.1080/10106049.2018.1489422

Pham, B.T., Shirzadi, A., Tien Bui, D., Prakash, I., Dholakia, M.B. 2018. A hybrid machine learning ensemble approach based on a Radial Basis Function neural network and Rotation Forest for landslide susceptibility modelling: A case study in the Himalayan area, India. *International Journal of Sediment Research 33*, 157–170. https://doi.org/10.1016/J.IJSRC.2017.09.008

Pourghasemi, H.R., Pradhan, B., Gokceoglu, C. 2012. Application of fuzzy logic and analytical hierarchy process (AHP) to landslide susceptibility mapping at Haraz watershed, Iran. *Natural Hazards 63*, 965–996. https://doi.org/10.1007/S11069-012-0217-2/FIGURES/4

Pradhan, A.M.S., Kim, Y.T. 2014. Relative effect method of landslide susceptibility zonation in weathered granite soil: A case study in Deokjeok-ri Creek, South Korea. *Natural Hazards 72*, 1189–1217. https://doi.org/10.1007/s11069-014-1065-z

Pradhan, B., Abokharima, M.H., Jebur, M.N., Tehrany, M.S. 2014. Land subsidence susceptibility mapping at Kinta Valley (Malaysia) using the evidential belief function model in GIS. *Natural Hazards 73*, 1019–1042. https://doi.org/10.1007/S11069-014-1128-1/FIGURES/4

Rane, P.R., Vincent, S. 2022. Landslide Susceptibility Mapping Using Machine Learning Algorithms for Nainital, India. *Engineered Science 17*, 142–155. https://doi.org/10.30919/es8d600

Reis, S., Yalcin, A., Atasoy, M., Nisanci, R., Bayrak, T., Erduran, M., Sancar, C., Ekercin, S. 2012. Remote sensing and GIS-based landslide susceptibility mapping using frequency ratio and analytical hierarchy methods in Rize province (NE Turkey). *Environmental Earth Sciences 66*, 2063–2073. https://doi.org/10.1007/s12665-011-1432-y

Saha, S., Roy, J., Hembram, T.K., Pradhan, B., Dikshit, A., Abdul Maulud, K.N., Alamri, A.M. 2021. Comparison between deep learning and tree-based machine learning approaches for landslide susceptibility mapping. *Water 13*. https://doi.org/10.3390/w13192664

Saha, S., Roy, J., Pradhan, B., Hembram, T.K. 2021. Hybrid ensemble machine learning approaches for landslide susceptibility mapping using different sampling ratios at East Sikkim Himalayan, India. *Advances in Space Research 68*, 2819–2840. https://doi.org/10.1016/j.asr.2021.05.018

Sahin, E.K., Colkesen, I., Kavzoglu, T. 2018. A comparative assessment of canonical correlation forest, random forest, rotation forest and logistic regression methods for landslide susceptibility mapping. *Geocarto International 35 (4)*, 341–363. https://doi.org/10.1080/10106049.2018.1516248

Sarkar, S., Roy, A.K., Martha, T.R. 2013. Landslide susceptibility assessment using Information Value Method in parts of the Darjeeling Himalayas. *Journal of the Geological Society of India 82*, 351–362. https://doi.org/10.1007/S12594-013-0162-Z/METRICS

Shmuel, A., Heifetz, E. 2022. Global Wildfire Susceptibility Mapping Based on Machine Learning Models. *Forests 13*, 1050. https://doi.org/10.3390/F13071050

Taheri, K., Shahabi, H., Chapi, K., Shirzadi, A., Gutiérrez, F., Khosravi, K. 2019. Sinkhole susceptibility mapping: A comparison between Bayes-based machine learning algorithms. *Land Degradation & Development 30*, 730–745. https://doi.org/10.1002/LDR.3255

Teerarungsigul, S., Torizin, J., Fuchs, M., Kühn, F., Chonglakmani, C. 2016. An integrative approach for regional landslide susceptibility assessment using weight of evidence method: a case study of Yom River Basin, Phrae Province, Northern Thailand. *Landslides 13*, 1151–1165. https://doi.org/10.1007/S10346-015-0659-1

Vapnik, V. 1995. The Nature of Statistical Learning Theory. https://books.google.com.tr/books?hl=tr&lr=&id=sna9BaxVbj8C&oi=fnd&pg=PR7&dq=The+nature+of+statistical+learning+theory:Springer+science+and+business+media&ots=oqM9O-hse7&sig=4QK9MXnmvVEX84JC-kDF4dwCArI&redir_esc=y#v=onepage&q=The nature of statistical lea.

Varnes, D.J. 1984. Landlisde hazard zonation: a review of principles and practice. *Natural Hazards 23*, 13–14.

Wang, Z., Liu, Q., Liu, Y. 2020. Mapping landslide susceptibility using machine learning algorithms and GIS: A case study in Shexian county, Anhui province, China. *Symmetry 12*, 1–18. https://doi.org/10.3390/sym12121954

Wilson, J.P., Gallant, J.C. 2000. Terrain analysis : principles and applications, edited by John P. Wilson, John C. Gallant, 520.

Wu, Y., Ke, Y., Chen, Z., Liang, S., Zhao, H., Hong, H. 2020. Application of alternateng decision tree with AdaBoost and bagging ensembles for landslide susceptibility mapping. *Catena 187*, 104396. https://doi.org/10.1016/J.CATENA.2019.104396

Xie, W., Li, X., Jian, W., Yang, Y., Liu, H., Robledo, L.F., Nie, W. 2021. A novel hybrid method for landslide susceptibility mapping-based geodetector and machine learning cluster: A case of Xiaojin County, China. *ISPRS International Journal of Geo-Information 10*. https://doi.org/10.3390/ijgi10020093

Yalcin, A. 2008. GIS-based landslide susceptibility mapping using analytical hierarchy process and bivariate statistics in Ardesen (Turkey): Comparisons of results and confirmations. *Catena 72*, 1–12. https://doi.org/10.1016/J.CATENA.2007.01.003

Yong, C., Jinlong, D., Fei, G., Bin, T., Tao, Z., Hao, F., Li, W., Qinghua, Z. 2022. Review of landslide susceptibility assessment based on knowledge mapping. *Stochastic Environmental Research and Risk Assessment* 0123456789. https://doi.org/10.1007/s00477-021-02165-z

Youssef, A.M., Pourghasemi, H.R. 2021. Landslide susceptibility mapping using machine learning algorithms and comparison of their performance at Abha Basin, Asir Region, Saudi Arabia. *Geoscience Frontiers 12*, 639–655. https://doi.org/10.1016/j.gsf.2020.05.010

Youssef, A.M., Pourghasemi, H.R., Pourtaghi, Z.S., Al-Katheeri, M.M. 2016. Landslide susceptibility mapping using random forest, boosted regression tree, classification and regression tree, and general linear models and comparison of their performance at Wadi Tayyah Basin, Asir Region, Saudi Arabia. *Landslides 13*, 839–856. https://doi.org/10.1007/S10346-015-0614-1/FIGURES/12

Zhou, C., Yin, K., Cao, Y., Ahmed, B., Li, Y., Catani, F., Pourghasemi, H.R. 2018. Landslide susceptibility modelling applying machine learning methods: A case study from Longju in the Three Gorges Reservoir area, China. *Computers and Geosciences 112*, 23–37. https://doi.org/10.1016/j.cageo.2017.11.019